

# The neutron star soft X-ray transient 1H 1905+000 in quiescence

P.G. Jonker<sup>1,2,3\*</sup>, C.G. Bassa<sup>3</sup>, G. Nelemans<sup>4</sup>, A.M. Juett<sup>5</sup>, E.F. Brown<sup>6</sup>, D. Chakrabarty<sup>7</sup>

<sup>1</sup>SRON, National Institute for Space Research, Sorbonnelaan 2, 3584 CA, Utrecht, The Netherlands

<sup>2</sup>Harvard-Smithsonian Center for Astrophysics, 60 Garden Street, Cambridge, MA 02138, Massachusetts, U.S.A.

<sup>3</sup>Astronomical Institute, Utrecht University, P.O.Box 80000, 3508 TA, Utrecht, The Netherlands

<sup>4</sup>Department of Astrophysics, IMAPP, Radboud University Nijmegen, Toernooiveld 1, 6525 ED, Nijmegen, The Netherlands

<sup>5</sup>Department of Astronomy, University of Virginia, Charlottesville, VA 22903, U.S.A.

<sup>6</sup>Department of Physics and Astronomy, Michigan State University, East Lansing, MI 48824, U.S.A.

<sup>7</sup>Department of Physics and Kavli Institute for Astrophysics and Space Research, Massachusetts Institute of Technology, Cambridge, MA 02139, U.S.A.

30 September 2018

## ABSTRACT

In this Paper we report on our analysis of a  $\sim 25$  ksec. *Chandra* X-ray observation of the neutron star soft X-ray transient (SXT) 1H 1905+000 in quiescence. Furthermore, we discuss our findings of the analysis of optical photometric observations which we obtained using the Magellan telescope and photometric and spectroscopic observations which we obtained using the Very Large Telescope at Paranal. The X-ray counterpart of 1H 1905+000 was not detected in our *Chandra* data, with a 95 per cent confidence limit to the source count rate of  $1.2 \times 10^{-4}$  counts s<sup>-1</sup>. For different spectral models this yields an upper limit on the luminosity of  $1.8 \times 10^{31}$  erg s<sup>-1</sup> (for an upper limit on the distance of 10 kpc.) This luminosity limit makes 1H 1905+000 the faintest neutron star SXT in quiescence observed to date. The neutron star luminosity is so low that it is similar to the lowest luminosities derived for black hole SXTs in quiescence. This low luminosity for a neutron star SXT challenges the hypothesis presented in the literature that black hole SXTs in quiescence have lower luminosities than neutron star SXTs as a result of the presence of a black hole event horizon. Furthermore, the limit on the neutron star luminosity obtained less than 20 years after the outburst has ceased, constrains the thermal conductivity of the neutron star crust. Finally, the neutron star core must be so cold that unless the time averaged mass accretion rate is lower than  $2 \times 10^{-12} M_{\odot}$  yr<sup>-1</sup>, core cooling has to proceed via enhanced neutrino emission processes. The time averaged mass accretion rate can be derived from binary evolution models if the orbital period of the system is known. Our optical observations show that the optical counterpart discovered when the source was in outburst has faded. Near the outburst optical position we find two stars with a separation of 0.7'' and  $I=19.3 \pm 0.1$  and  $21.3 \pm 0.1$ . VLT optical spectroscopy revealed that the spectrum of the brighter of the two sources is a G5–7V–star. However, the outburst astrometric position of the optical counterpart does not coincide with the position of the G5–7V–star nor with that of the fainter star. We derive a limit on the absolute I-band magnitude of the quiescent counterpart of  $M_I > 7.8$  assuming the source is at 10 kpc. This is in line with 1H 1905+000 being an ultra-compact X-ray binary, as has been proposed based on the low outburst V-band absolute magnitude.

**Key words:** stars: individual (1H 1905+000) — accretion: accretion discs — stars: binaries — stars: neutron — X-rays: binaries

\* email : p.jonker@sron.nl. Based on observations made with

## 1 INTRODUCTION

Low-mass X-ray binaries are binary systems in which a  $\lesssim 1M_{\odot}$  star transfers matter to a neutron star or a black hole. A large fraction of the low-mass X-ray binaries are transient systems – the so called soft X-ray transients (SXTs; e.g. see Chen et al. 1997). Before the launch of the XMM-Newton and *Chandra* satellites only a few (mostly) nearby SXTs could be studied in quiescence (e.g. the black hole candidates A 0620–00 and V404 Cyg and the neutron star systems Cen X-4 and Aql X-1; Wagner et al. 1994; McClintock et al. 1995; van Paradijs et al. 1987). Using the XMM-Newton and *Chandra* satellites many more systems were studied in quiescence in the initial years of operation (see e.g. Garcia et al. 2001, Kong et al. 2002, Rutledge et al. 2002b, Wijnands et al. 2001, Campana et al. 2002, Hameury et al. 2003, Jonker et al. 2004). Contemporaneous theoretical progress provided the framework for the interpretation of these observations (Narayan & Yi 1994, Narayan et al. 1997; Brown et al. 1998, Colpi et al. 2001; Zavlin et al. 1996; Gängsche et al. 2002) which turned out to have a profound impact on two important areas of high energy astrophysics.

First, comparing the quiescent luminosity of neutron star SXTs with that of black hole SXTs it was found that black hole (BH) SXTs are systematically fainter in quiescence than neutron stars (Narayan et al. 1997, Menou et al. 1999, Garcia et al. 2001, Kong et al. 2002). This has been interpreted as evidence for advection of energy across a BH event horizon. If true this would constitute the first confirmation of a prediction of Einstein’s Theory of General Relativity in the strong field regime. Despite many objections to this interpretation (Campana & Stella 2000; Abramowicz et al. 2002), alternative explanations for the difference in quiescent luminosity (Fender et al. 2003), and neutron stars which turned out to be fainter than initially found to be the rule (e.g. SAX J1808.4–3658, Campana et al. 2002; EXO 1747–214; Tomsick et al. 2005), none of the neutron star SXTs have quiescent luminosities as low as the faintest BH SXTs, which have 0.5–10 keV luminosities  $< 10^{31}$  erg s $^{-1}$ ; (e.g. Kong et al. 2002, Hameury et al. 2003). Hence, irrespective of the interpretation, the difference in quiescent luminosity between BH and neutron star SXTs seems to be one of the very few distinct characteristics between BHs and neutron stars.

Secondly, the quiescent spectra of neutron star SXTs are well-fit by a neutron star atmosphere model (NSA) sometimes supplemented with a power-law component. Especially in sources with a quiescent luminosity near  $10^{33}$  erg s $^{-1}$  the spectrum is dominated by a strong thermal component (Jonker et al. 2004). The thermal component is thought to be due to the hot neutron star core moderated by the neutron star atmosphere. The neutron star core temperature can be calculated by combining well established theories about the time-averaged mass accretion rates in neutron star SXTs (Kraft et al. 1962; Verbunt & van den Heuvel 1995), the pycnonuclear reactions taking place in the neutron star crust (Salpeter & van Horn 1969; Haensel & Zdunik 1990; Kitamura 2000) and theoretical neutron star cooling predictions (see Yakovlev & Pethick 2004 for a review). Therefore, in theory, an NSA-fit provides means to measure the mass

and radius of the neutron star and hence constrain the equation of state (EoS) of matter at supranuclear densities. The description of the relations between pressure and density of matter (the EoS) under the extreme conditions encountered in neutron stars is one of the ultimate goals of the study of neutron stars.

In practice, numbers typical for a canonical neutron star were found (e.g. Heinke et al. 2003), rendering support for this interpretation. However, there is an ongoing debate whether the temperature of the thermal (NSA) component is varying on short timescales (cf. Rutledge et al. 2002a, Campana et al. 2004, and Jonker et al. 2005). Small temperature changes could be explained by changes in the neutron star atmosphere due to ongoing low-level accretion (Brown et al. 2002). Large changes on short timescales would render it unlikely that the soft/thermal component is due to cooling of the neutron star, limiting the applicability of the NSA model fit. Finally, there are currently two sources known which returned to quiescence after a several year-long accretion epoch (i.e. KS 1731–260 and MXB 1659–298). As a result of these long accretion episodes the neutron star *crust* is heated to temperatures larger than that of the core. The observed thermal spectral component has been identified as cooling of the neutron star crust (Wijnands et al. 2002; Rutledge et al. 2002b). As the crust cools the X-ray spectral properties also change slightly (Wijnands et al. 2004).

Recent *Chandra* observations of accretion powered millisecond X-ray pulsars in quiescence found that the quiescent luminosity of many of those observed so far, not just SAX J1808.4–3658, is low (Wijnands et al. 2005; Campana et al. 2005). A possible exception could be the accretion-powered millisecond X-ray pulsar IGR J00291+5934 (Jonker et al. 2005). Furthermore, the X-ray spectrum is in most cases dominated by a power-law component similar to that of quiescent BH (Wijnands et al. 2005). Hence, the dichotomy between the BH and neutron star quiescent luminosity may not be as large as previously derived (see also Jonker & Nelemans 2004). We note however, that reliable distance estimates could be made for only 2 accretion powered millisecond systems, SAX J1808.4–3658 and XTE J1814–338 (in’t Zand et al. 2001; Strohmayer et al. 2003). For the other systems the distance estimates are rather uncertain, making the quiescent luminosity uncertain as well. The low-luminosity and the small contribution of a thermal spectral component to the luminosity of SAX J1808.4–3658 (<10%; Campana et al. 2002, although see the comment about this upper limit in Yakovlev et al. 2005) hint at a massive neutron star ( $M > 1.7M_{\odot}$ ; Yakovlev et al. 2003, Yakovlev & Pethick 2004). The upper limit on the thermal spectral component implies that the neutron star core of SAX J1808.4–3658 must release the energy produced in the crust due to pycnonuclear reactions rapidly via enhanced neutrino emission. This enhanced neutrino emission can only occur when the neutron star mass is larger than the canonical  $1.4 M_{\odot}$ .

1H 1905+000 was first detected on MJD 42368 (UTC) by Ariel 5 (Seward et al. 1976). Six type I X-ray bursts were discovered on different occasions by SAS-3 firmly establishing the nature of the compact object as a neutron star (Lewin et al. 1976). The last reported detection of the source was that by EXOSAT on MJD 46316 (UTC).

A radius expansion burst was detected on this occasion (Chevalier & Ilovaisky 1990). During the period of activity the source has also been detected with HEAO-1 and Einstein (Reid et al. 1980 and Christian & Swank 1997, respectively). However, the source was not detected in the ROSAT All Sky Survey (Juett & Chakrabarty 2005). The source likely went to quiescence at the end of the 1980s/early 1990s. Next, 1H 1905+000 was observed for 5 ks with the back-illuminated S3 CCD-chip of the Advanced CCD Imaging Spectrometer (ACIS) detector on board the *Chandra* satellite with the High-Energy Transmission Grating inserted (Juett & Chakrabarty 2005). Again no source was detected at the position of the optical counterpart discovered when the source was in outburst (Chevalier et al. 1985). The derived upper limit on the unabsorbed 0.5–10 keV flux for 1H 1905+000 was  $1 \times 10^{-14}$  erg cm $^{-2}$  s $^{-1}$  for an assumed black body spectrum with a temperature of 0.3 keV. The distance for 1H 1905+000 derived from the observed radius expansion burst peak flux is 7.3 or 10 kpc (Jonker & Nelemans 2004; the values assume hydrogen and helium bursts, respectively). From Einstein observations Christian & Swank (1997) determined that the interstellar extinction,  $N_H$ , to 1H 1905+000 is  $(1.9 \pm 0.2) \times 10^{21}$  cm $^{-2}$ . This yields an upper limit to the intrinsic (i.e. corrected for the interstellar extinction) 0.5–10 keV source luminosity of  $1.0 - 1.7 \times 10^{32}$  erg s $^{-1}$  for 1H 1905+000. In summary, it is likely that the source had been accreting steadily at  $L \sim 4 \times 10^{36}$  erg s $^{-1}$  for more than 10 years before returning to quiescence. In this Paper we present our analysis of a  $\sim 25$  ksec. *Chandra* observation of this neutron star SXT in quiescence. Furthermore, our analysis of Very Large Telescope and Magellan optical observations of the region of the source in quiescence is also presented.

## 2 OBSERVATIONS, ANALYSIS AND RESULTS

### 2.1 Optical Magellan, VLT, archival WHT and CFHT observations

In order to determine the best (optical) position of 1H 1905+000 and to search for the optical counterpart in quiescence, we have obtained I-band images with exposure times of 10 seconds and 2x300 seconds using the Inamori-Magellan Areal Camera and Spectrograph (IMACS) instrument mounted on the 6.5 m Magellan-Baade telescope on July 7, 2005, 03:03 UTC (MJD 53558.14594 UTC). The seeing was 0.69''. Using the second USNO CCD Astrograph Catalog (UCAC2) catalogue (Zacharias et al. 2004) we determined the position of 71 bright, unsaturated, stars in the 10-second IMACS image to obtain an astrometric solution (the rms of the fit was 0''.060 both in right ascension [ $\alpha$ ] and in declination [ $\delta$ ]). Subsequently, the astrometric solution of the 10-second frame was transferred to the 300-second images using 1397 stars. In this the uncertainty was 0''.017 in  $\alpha$  and 0''.015 in  $\delta$ . Hence, the absolute uncertainty in the optical astrometry of the 300 second images is 0''.062 in  $\alpha$  and 0''.061 in  $\delta$ . Next, standard image processing was done in MIDAS (i.e. bias subtraction and flatfield correction.) The two 300 seconds observations were averaged (see Fig. 1). We have observed standard stars on the same CCD close in time and airmass to the IMACS observations of 1H 1905+000.

Using point spread function fitting (psf-fitting) techniques we found that the star present near the optical position of the counterpart discovered in outburst consists of two stars close together (within 0.7'') with I-band magnitudes  $19.3 \pm 0.1$  (star A) and  $21.3 \pm 0.1$  (star D; see Fig. 2). Star A has a position  $\alpha_{J2000.0} = 19^{\text{h}}08^{\text{m}}27^{\text{s}}.217 \pm 0''.063$ ,  $\delta_{J2000.0} = +00^{\circ}10'09''.42 \pm 0''.062$ . Star D has a position  $\alpha_{J2000.0} = 19^{\text{h}}08^{\text{m}}27^{\text{s}}.171 \pm 0''.063$ ,  $\delta_{J2000.0} = +00^{\circ}10'09''.29 \pm 0''.062$  (68 per cent confidence uncertainty; the uncertainty in this position is the square root of the quadratically added internal uncertainty [0''.01 in both  $\alpha$  and  $\delta$ ] and the uncertainty in the absolute calibration of the astrometric solution mentioned earlier). As a (conservative) limit on the detection limit of the 2x300 second I-band image we determined the magnitude of the faintest star detected at 5  $\sigma$ ; it has I=23.5.

We have also obtained 14 white light images with the FOcal Reducer and low dispersion Spectrograph 2 (FORS2) mounted on the 8.2 m Very Large Telescope (VLT) Yepun (images were obtained on MJD 53135.3668, 53135.3714, 53143.3471, 53143.3504, 53144.1639, 53146.3858, 53146.3901, 53148.2501, 53148.2555, 53148.2656, 53148.2665, 53148.302, 53148.3606, 53148.3624 UTC). Each of these images has an exposure time of 10 seconds. We corrected for bias using the overscan region of the CCD, however, no white light flatfield images are available since these images were acquisition images for spectroscopic observations (see below). Therefore, we could not correct for pixel-to-pixel variations in sensitivity. We used psf-fitting in order to determine the relative brightness of the two stars present close to the position of the optical counterpart in outburst (see Fig. 2). We were able to use 12 out of the 14 acquisition observations for which the seeing conditions were 0.45''–0.82'' to search for white light variability. The rms scatter in the magnitude of star D is 0.11 magnitudes. However, this variability could have been introduced by the psf-fitting technique since the rms variability in the fainter of the two stars in another star-pair of similar brightness ratio and separation was 0.09 magnitudes. We conclude that star D did not vary significantly over the course of our observations. We median combined six of the 10 seconds images with the best seeing (seeing  $< 0.6''$ ). Next, we again used the UCAC2 catalogue (Zacharias et al. 2004) to determine the position of 23 bright, unsaturated, stars in the resultant image to obtain an astrometric solution (the rms of the fit was 0''.063 in  $\alpha$  and 0''.082 in  $\delta$ . The position of star A and D are consistent with being the same as during the IMACS observations.

As mentioned above the white light images are acquisition images for spectroscopic observations. We have obtained VLT/FORS2 spectra of star A (cf. Fig. 1 & 2) using the 600B and 600RI gratings with an exposure time of  $\sim 2750$  seconds on MJD 53146.4006, 53148.3059, 53148.3659 and MJD 53135.3744, 53143.3541, 53143.3883, 53148.2690, respectively. Hence, the total exposure in the 600B grating spectrum was  $\sim 2.3$  hours and in the 600RI grating spectrum it was  $\sim 3.05$  hours. A slit width of 1'' was used on each occasion. The dispersion was  $1.5 \text{ \AA pixel}^{-1}$  at  $4429 \text{ \AA}$  with the 600B grating and  $1.65 \text{ \AA pixel}^{-1}$  at  $6552 \text{ \AA}$  with the 600RI grating. With a slit width of 1'', the spectral resolution varies from approximately  $400 \text{ km s}^{-1}$  at  $4430 \text{ \AA}$  to  $300 \text{ km s}^{-1}$  at  $6550 \text{ \AA}$ . The spectra were extracted and reduced using

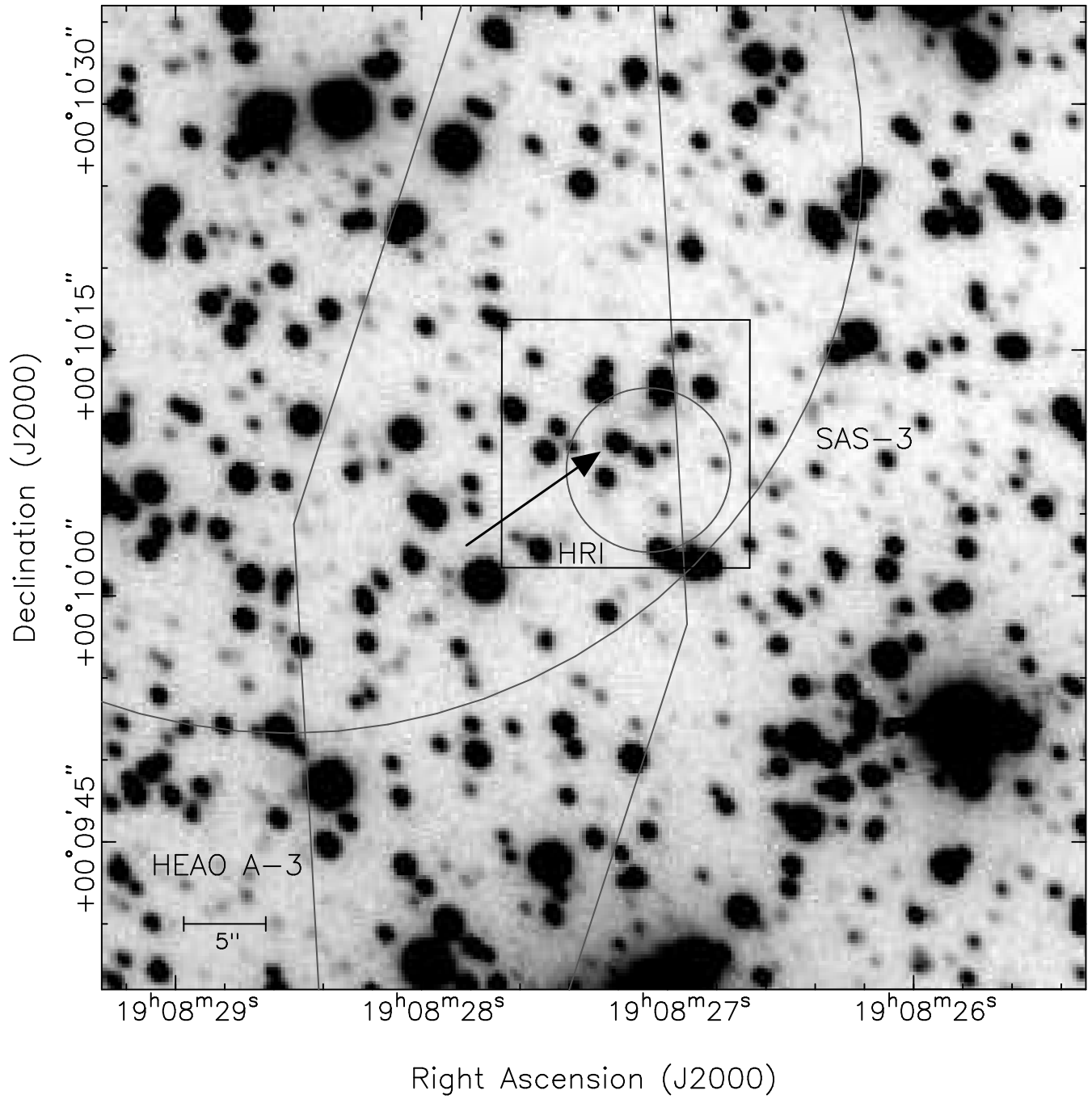


**Figure 1.** An I-band finder chart of the field of 1H 1905+000 obtained by median combining the two 300 seconds images obtained with Magellan/IMACS (1'x1', North is up and East is left). Overplotted are the HEAO A-3 (diamond shape), the Einstein HRI (small circle) and the SAS-3 (large circle) error regions. The box shows the region plotted in Figure 2. The arrow indicates the approximate position of the blue counterpart discovered when 1H 1905+000 was in outburst (Chevalier et al. 1985.) Psf-fitting showed that this star consists of two stars separated by 0.7'' (see Figure 2).

IRAF<sup>1</sup>. Once the spectra were reduced the spectral analysis was done using MOLLY. The spectrum of this star is consistent with a G5–7V star (see Fig. 3).

We have median combined 14 archival V-band observations of the field of 1H 1905+000 obtained with the AUX

port camera mounted on the 4.2 m William Herschel Telescope located at the Roque de Los Muchachos Observatory, La Palma, Spain on July 30, 1994 (MJD 49563 UTC). These images have been retrieved from the ING Archive. In total 100 images had been obtained but we only selected the 14 with best seeing conditions (seeing <0.8''). The G-star is detected at a magnitude  $V=20.61\pm0.01$  (statistical error only) and star D is barely detected at  $V=23.3\pm0.1$ . We note

<sup>1</sup> IRAF is distributed by the National Optical Astronomy Observatories

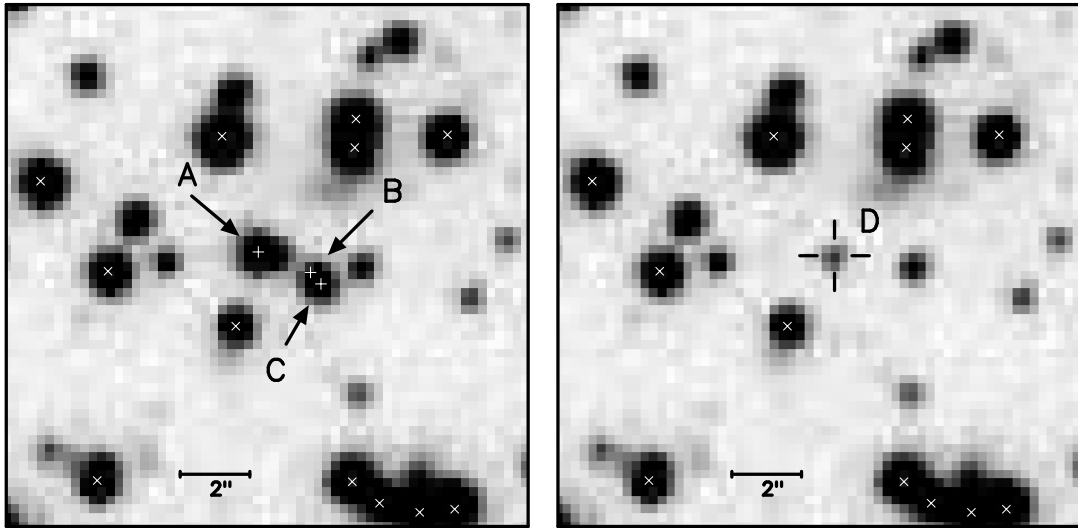


**Figure 2.** *Left:* A median combined image of six 10 seconds VLT FORS2 white light observations of 1H 1905+000 obtained under excellent seeing conditions ( $< 0.6''$ ). *Right:* The three stars (A,B,C) indicated with a small, white plus sign in the *left* image have been subtracted using psf-fitting. A star very close to the position of the optical counterpart in outburst remains (we call this star D).

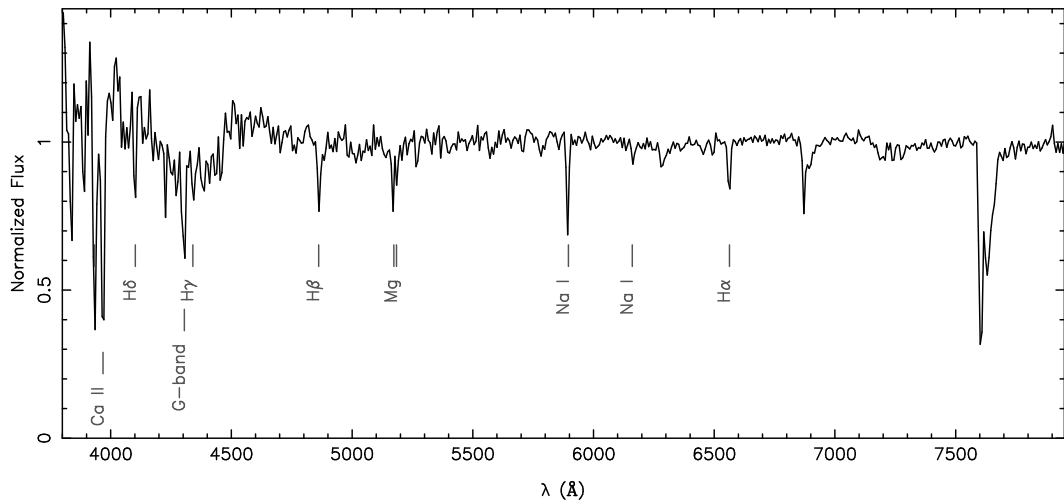


**Figure 3.** The combined, normalised VLT FORS2 600B (2.3 hours total exposure) and 600RI (3.05 hours total exposure) grating spectrum of the star at the position of the outburst optical counterpart of 1H 1905+000. The spectrum resembles that of a G5–7V-star.

however that only one standard star was observed and only one filter was obtained. Hence, colour corrections could be important (these systematic uncertainties are not included). The positions of both sources is consistent with that derived from the IMACS images.

Finally, we have obtained a subsection ( $37'' \times 37''$ ) of the 1984  $V$ -band outburst Canada–France–Hawaii Telescope (CFHT) image published by Chevalier et al. (1985; Illovaiky 2005, priv. comm.). We have astrometrically tied this image to the 10s IMACS  $I$ -band image. The uncertainty in the tie is  $0''.050$  in  $\alpha$  and  $0''.055$  in  $\delta$ . Although the resolution of the image is worse than that of the FORS2 and IMACS images, it is clear that there is excess emission compared to that attributable to stars at the position of star A and D (Fig. 5). Using a Gaussian for the psf of the outburst image, we have fitted the stars on the image with the aim to determine the position of the source in outburst taking into

account the flux from star A and D. The positions of the stars in the IMACS  $I$ -band observations were transformed to the CFHT image and kept fixed during the fitting process. As such, we only fitted for the overall background, the fluxes of the IMACS stars and the flux and position of the source in outburst. For the latter we obtain  $\alpha = 19^{\mathrm{h}}08^{\mathrm{m}}27.200$ ,  $\delta = +00^{\circ}10'09''.10$ . Here, the intrinsic uncertainty on the source position is  $0''.03$  in both  $\alpha$  and  $\delta$ . For the absolute uncertainty this should be quadratically added to the uncertainties of the ties between the CFHT  $V$ -band and IMACS  $I$ -band image (see above) and the IMACS  $I$ -band image and the UCAC2 catalog ( $0''.060$  in both  $\alpha$  and  $\delta$ ). However, for comparison of the outburst position with that of star A and D, we can directly compare the outburst position with the positions on the 5 min IMACS  $I$ -band image. For this, we can neglect the IMACS–UCAC2 uncertainty, but must include the uncertainty in the tie between the 10 sec and 5 min

IMACS images ( $0.^{\prime\prime}017$  in  $\alpha$  and  $0.^{\prime\prime}015$  in  $\delta$ ). As such, star A is offset from the outburst position by  $-0.^{\prime\prime}255 \pm 0.^{\prime\prime}062$  in  $\alpha$  and  $-0.^{\prime\prime}320 \pm 0.^{\prime\prime}065$  in  $\delta$ , while star D is offset by  $0.^{\prime\prime}435 \pm 0.^{\prime\prime}062$  and  $-0.^{\prime\prime}190 \pm 0.^{\prime\prime}065$ . These offsets correspond to  $4.5\sigma$  for star A and  $5.3\sigma$  for star D. In Fig. 5 we have overplotted with small crosses the position of several reference stars detected in Fig. 2 and with a small circle the position of the outburst optical counterpart. As can be seen it is unlikely that the outburst counterpart can be associated with star D unless that star has a high proper motion of 24 milliarcseconds year $^{-1}$ . At a distance of 10 kpc this would convert into a rather large velocity of  $\sim 1100$  km s $^{-1}$ . Finally, we have investigated whether the differential Galactic rotation at  $l^{ii} = 35^{\circ}$  can be used to explain the observed offset of star D from the outburst optical position, under the assumption that star D arises due to the companion star and/or accretion disc of 1H 1905+000 at 10 kpc or at 7.5 kpc. The change in position with respect to other field stars is less than  $0.1''$  over the 20 year that separate the CFHT V-band outburst observations and the Magellan I-band observations. This is insufficient to explain the observed offset. We conclude that star D is not the quiescent optical counterpart to 1H 1905+000.

As mentioned above, the G-star contributes significantly to the outburst V-band magnitude measured by Chevalier et al. (1985). We used the properties of the G5–7V star and the V and I-band magnitudes observed when the low-mass X-ray binary was in quiescence to determine the G-star distance. In this we follow Chevalier et al. (1985) who noted that the interstellar extinction does not increase significantly in the direction of 1H 1905+000 for sources with a distance larger than 4 kpc. Hence, we used the same  $N_H$  for the G-star as was found for 1H 1905+000 in outburst. We used Rieke & Lebofsky (1985) to convert  $N_H$  to an  $A_V$  and the tables of Schlegel et al. (1998) to convert  $A_V$  to  $A_U$ ,  $A_B$  and  $A_I$ . We corrected the observed magnitudes for the interstellar extinction and plotted the optical SED for the outburst source as well as for the G-star (see Figure 4). To indicate the contribution of the outburst accretion disc, we included in the plot the SED contribution of a small, spherical, hot component. For the G-star we find a distance of 8.5 kpc (fixing the radius to  $1 R_{\odot}$ ), for the accretion disc we took 10 kpc for its distance and we get a radius of  $\approx 0.08 R_{\odot}$  for a temperature of  $3 \times 10^4$  K. Such a temperature is in the range of temperatures found for accretion discs around low-mass X-ray binaries (see for instance van Paradijs & McClintock 1995 and references therein). The fact that only such a small disc can be accommodated adds to the evidence that 1H 1905+000 is an ultra-compact X-ray binary.

## 2.2 *Chandra* X-ray observations

We observed 1H 1905+000 with the back-illuminated S3 CCD-chip of the Advanced CCD Imaging Spectrometer (ACIS) detector on board the *Chandra* satellite. The observations started on MJD 53425.852665 (UTC; Feb. 24, 2005). The net, on-source exposure time was  $\sim 24.8$  ks. The data telemetry mode was set to *very faint* to allow for a better background subtraction. After the data were processed by the *Chandra* X-ray Center (ASCDS version 7.5.0), we analysed them using the *CIAO 3.2.1* software developed by the *Chandra* X-ray Center. We reprocessed the data to clean

the background and take full advantage of the *very faint* data mode. We searched the data for background flares but none were found, hence we used all data in our analysis. We detect three sources in the field of view of the ACIS S3 CCD.

Since one of the detected X-ray sources (source 1 below) has an optical counterpart detectable in our FORS2 white light images, we use the accurate optical position of this source to apply a boresight correction to the *Chandra* observation and hence improve the astrometric accuracy of the *Chandra* observation. The boresight shift that we find is:  $\Delta\alpha = -0.^{\prime\prime}210 \pm 0.^{\prime\prime}071$ ,  $\Delta\delta = +0.^{\prime\prime}080 \pm 0.^{\prime\prime}088$ . The J2000.0  $\alpha$  and  $\delta$  of the three detected X-ray sources are:

- (1)  $\alpha_{J2000.0} = 19^{\text{h}}08^{\text{m}}34^{\text{s}}.094$ ,  $\delta_{J2000.0} = +00^{\circ}11'39.^{\prime\prime}09$  (with an error of  $0.^{\prime\prime}078$  in  $\alpha$  and  $0.^{\prime\prime}094$  in  $\delta$ )
- (2)  $\alpha_{J2000.0} = 19^{\text{h}}08^{\text{m}}22^{\text{s}}.183$ ,  $\delta_{J2000.0} = +00^{\circ}07'33.^{\prime\prime}65$  (with an error of  $0.^{\prime\prime}11$  in  $\alpha$  and  $0.^{\prime\prime}12$  in  $\delta$ )
- (3)  $\alpha_{J2000.0} = 19^{\text{h}}08^{\text{m}}19^{\text{s}}.878$ ,  $\delta_{J2000.0} = +00^{\circ}06'18.^{\prime\prime}20$  (with an error of  $0.^{\prime\prime}13$  in  $\alpha$  and  $0.^{\prime\prime}15$  in  $\delta$ ).

We assign the following names to these sources CXOU J190834.1+001139, CXOU J190822.2+000734, CXOU J190819.9+000618, respectively. The X-ray source closest to the position of the optical counterpart found in outburst (Chevalier et al. 1985) is more than 2 arcminutes away. We do not detect a source at the position of the optical outburst source as measured in the CFHT V-band image in our  $\sim 25$  ks-long *Chandra* observation. Furthermore, we detect no X-ray photons within a  $1''$  circle centred on the optical outburst position. Following Gehrels (1986), we take an upper limit of 3 source photons to determine the  $\sim 95$  per cent upper limit on the source count rate of  $1.2 \times 10^{-4}$  counts s $^{-1}$ . We used PIMMS version 3.6a<sup>2</sup> to estimate upper limits on the source flux for a given interstellar extinction and an (assumed) spectral energy distribution for the source. In Table 1 we give these upper limits to the unabsorbed 0.5–10 keV source flux and 0.5–10 keV source luminosity.

## 3 DISCUSSION

We have observed the field of the neutron star SXT 1H 1905+000 in X-rays with the *Chandra* satellite for  $\sim 25$  ksec, but did not detect the source in quiescence. Depending on the assumed spectral energy distribution, the interstellar extinction, and the distance we derive an upper limit to the 0.5–10 keV luminosity for 1H 1905+000 of  $L_{0.5-10\text{keV}, d=10\text{kpc}} < 1.8 \times 10^{31} \text{ ergs}^{-1}$  whereas,  $L_{0.5-10\text{keV}, d=7.5\text{kpc}} < 1.0 \times 10^{31} \text{ ergs}^{-1}$ . If we assume a neutron star of radius 10 km and a neutron star atmosphere model as given by Zavlin et al. (1996) then the upper limit on the 0.5–10 keV luminosity can be converted to an upper limit on the effective temperature of  $T_{\text{eff}} < 7.5 \times 10^5$  K. These upper limits imply that the quiescent X-ray luminosity of 1H 1905+000 is the lowest of any neutron star SXT observed so far for which there is a reliable distance estimate. It was found earlier that the outburst absolute V-band magnitude of the system was 4 (assuming a distance of 10 kpc; Chevalier et al. 1985). Compared with other SXTs in outburst this is rather low,

<sup>2</sup> available at <http://cxc.harvard.edu/toolkit/pimms.jsp>

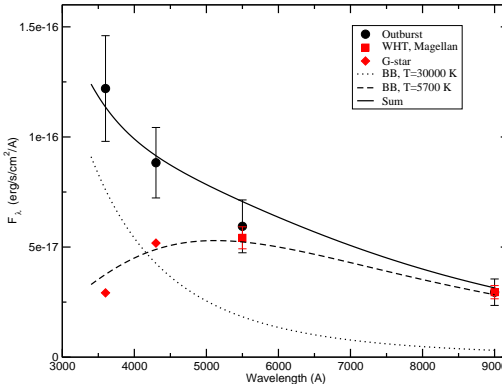


**Figure 4.** The optical spectral energy distribution of the outburst source and the G5–7 star. As can be seen the outburst SED can be explained as the superposition (solid line) of a hot, small black body component ( $T=30000$  K,  $R=0.08 R_{\odot}$ ; dotted line) and the G–star ( $T=5700$  K,  $R=1 R_{\odot}$ ; dashed line). Note that the lines (dotted, dashed and drawn) do not represent formal fits to the data points. The circles with error bars represent the dereddened optical outburst measurements (CFHT measurements; Chevalier et al. 1985). The squares are the dereddened observed magnitudes corresponding to the G–star when the low–mass X–ray binary was in quiescence (WHT and Magellan measurements; this work). The diamonds are the dereddened magnitudes derived using the observed spectral type and the source distance necessary to explain the G–star I–band magnitude.

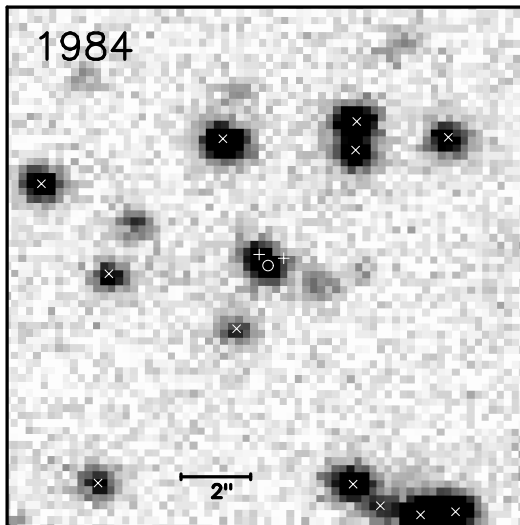


**Figure 5.** The 1984 CFHT V–band observation presented in Chevalier et al. (1985) with crosses overplotted on the reference stars and “+” signs on the G–star and star D. The outburst optical position depicted by a small circle is offset from both the centroid position of the G–star and that of star D.

which is typical for systems with orbital periods less than  $\sim 80$  minutes (also known as ultra–compact systems; see van Paradijs & McClintock 1994). Furthermore, from our optical Magellan/IMACS I–band observations of the system in quiescence and the precise astrometry we conclude that we do not detect the optical counterpart of 1H 1905+000 in quiescence, which for a distance of 10 kpc gives a limit on the absolute I–band magnitude of 1H 1905+000 in quiescence of  $M_I > 7.8$ . In this we took  $N_H = 1.9 \times 10^{21} \text{ cm}^{-2}$  as found during outburst, used Rieke & Lebofsky (1985) to convert  $N_H$  to an  $A_V$  and the tables of Schlegel et al. (1998) to convert  $A_V$  to  $A_I$ . Our conservative upper limit on the quiescent optical absolute magnitude is completely consistent with the proposed ultra–compact nature of 1H 1905+000. In order to fit observations the companion star has to be fainter than an M2 V star (Cox 2000). Hence, a (hot)

brown dwarf companion star such as that of SAX J1808.4–3658 (Bildsten & Chakrabarty 2001) would also be consistent with the current constraints.

The low quiescent X–ray luminosity of this source shows that the difference in the quiescent luminosity of black hole and neutron star SXTs found initially (e.g. Garcia et al. 2001) may have been a selection effect (see also Tomsick et al. 2005). The observations reported here show that at least some of the neutron star SXTs can be as faint as the faintest black hole SXTs in quiescence. The claim that the comparison between the black hole and neutron star luminosity in SXTs in quiescence provides evidence for a black hole event horizon is hence difficult to maintain. When comparing Eddington scaled neutron star and black hole luminosities, as has been done often in the literature, black hole SXTs are still less luminous than their

**Table 1.** Upper limits to the unabsorbed 0.5–10 keV source flux (F) and 0.5–10 keV luminosity (L) for various values of the interstellar extinction, different spectral energy distributions of the source, and using 7.5 and 10 kpc for the distance of 1H 1905+000. PL stands for power law, BB for blackbody.

$N_H$ $\text{cm}^{-2}$	Model	$F_{0.5-10 \text{ keV}}$ unabsorbed $\text{erg cm}^{-2} \text{ s}^{-1}$	$L_{0.5-10 \text{ keV}, d=10 \text{kpc}}$ $\text{erg s}^{-1}$	$L_{0.5-10 \text{ keV}, d=7.5 \text{kpc}}$ $\text{erg s}^{-1}$
1H 1905+000				
$2.1 \times 10^{21}$	PL index=2.0	$1.2 \times 10^{-15}$	$1.4 \times 10^{31}$	$8.1 \times 10^{30}$
$2.1 \times 10^{21}$	PL index=1.5	$1.5 \times 10^{-15}$	$1.8 \times 10^{31}$	$1.0 \times 10^{31}$
$2.1 \times 10^{21}$	BB temperature=0.2 keV	$8.3 \times 10^{-16}$	$9.9 \times 10^{30}$	$5.6 \times 10^{30}$
$2.1 \times 10^{21}$	BB temperature=0.3 keV	$7.3 \times 10^{-16}$	$8.7 \times 10^{30}$	$4.9 \times 10^{30}$
$1.9 \times 10^{21}$	PL index=2.0	$1.2 \times 10^{-15}$	$1.4 \times 10^{31}$	$7.8 \times 10^{30}$
$1.9 \times 10^{21}$	PL index=1.5	$1.5 \times 10^{-15}$	$1.8 \times 10^{31}$	$1.0 \times 10^{31}$
$1.9 \times 10^{21}$	BB temperature=0.2 keV	$7.8 \times 10^{-16}$	$9.4 \times 10^{30}$	$5.3 \times 10^{30}$
$1.9 \times 10^{21}$	BB temperature=0.3 keV	$7.0 \times 10^{-16}$	$8.4 \times 10^{30}$	$4.7 \times 10^{30}$
$1.7 \times 10^{21}$	PL index=2.0	$1.1 \times 10^{-15}$	$1.3 \times 10^{31}$	$7.5 \times 10^{30}$
$1.7 \times 10^{21}$	PL index=1.5	$1.5 \times 10^{-15}$	$1.7 \times 10^{31}$	$9.8 \times 10^{30}$
$1.7 \times 10^{21}$	BB temperature=0.2 keV	$7.4 \times 10^{-16}$	$8.8 \times 10^{30}$	$5.0 \times 10^{30}$
$1.7 \times 10^{21}$	BB temperature=0.3 keV	$6.7 \times 10^{-16}$	$8.0 \times 10^{30}$	$4.5 \times 10^{30}$

neutron star counterparts. The reasoning behind such a scaling stems from the notion that at orbital periods of the order of hours the gravitational wave radiation driven mass transfer rate for neutron stars and black holes is roughly similar when scaled to the Eddington rate *if the companion stars are main sequence stars* (Menou et al. 1999). However, for ultra-compact systems (as 1H 1905+000 likely is) the companion star cannot be a main sequence star making the Eddington scaling arbitrary. Furthermore, it is unclear whether the mass transfer rate set by the orbital period and the instantaneous mass accretion rate have a one-to-one correspondence in quiescent systems.

The low luminosity in quiescence can potentially be used together with the neutron star cooling theory to put constraints on the presence of condensates in the neutron star core (Yakovlev & Pethick 2004). Besides the core cooling mechanism we can constrain the thermal relaxation time and hence thermal conductivity of the neutron star crust. Since we do not detect the neutron star less than 20 years after the 11 year long outburst the neutron star crust must have a thermal relaxation time less than 20 years. However, presently the data does not allow us to distinguish between crustal conductivity set by electron–phonon conductivity (Baiko & Yakovlev 1995) or by electron–ion scattering (Yakovlev & Urpin 1980), since the inclusion of Cooper–pair neutrino emission in the crust alters the description considerably with respect to the status presented in Ushomirsky & Rutledge (2001) (e.g. see Yakovlev et al. 1999). Currently, less than 20 years after the outburst, the quiescent luminosity is determined by the core cooling processes again. However, to estimate the core temperature the average mass accretion rate over the last  $10^4$ – $10^5$  year has to be known (Colpi et al. 2001). This we can estimate from binary evolution theory. A primer for the evolutionary state of the low-mass X-ray binary (outside Globular Clusters) is the orbital period. In case of 1H 1905+000 the orbital period is unknown. However, as explained above, it is likely that 1H 1905+000 is an ultra-compact X-ray binary. The mass accretion rate for an ultra-compact system depends on the exact orbital period and the nature and age of the companion star but it can be as low as  $\sim 10^{-13} \text{ M}_\odot$

$\text{yr}^{-1}$  if the system is  $\sim 10$  Gyr old and if the orbital period is 60–90 minutes (e.g. Verbunt & van den Heuvel 1995, Deloye & Bildsten 2003, see also King & Wijnands 2006). If indeed the time averaged mass accretion rate is this low, the current limit on the luminosity does not provide a constraint on the core cooling. However, at such low mass transfer rates it might be difficult to feed an outburst that lasts longer than 11 years where the X-ray luminosity is  $\sim 4 \times 10^{36} \text{ erg s}^{-1}$  as in the case of 1H 1905+000.<sup>3</sup> In order to sustain such an accretion rate for 11 years the neutron star should have accreted  $\approx 4 \times 10^{-9} \text{ M}_\odot$ . If the mass transfer rate is  $10^{-13}/10^{-12} \text{ M}_\odot \text{ yr}^{-1}$  then it would take at least  $3.5 \times 10^4/3.5 \times 10^3$  year to build-up the accretion disc. In both cases this is a significant fraction of the core heating timescale. Brown et al. (1998) showed that in such a case the fraction of the heat released deep in the crust that is used to heat the core is smaller than 1. Assuming that the fraction is not less than 0.1 in 1H 1905+000 then, following Brown et al. (1998) we derive that for a time averaged mass accretion rate larger than  $2 \times 10^{-12} \text{ M}_\odot \text{ yr}^{-1}$ , enhanced neutrino emission processes must be operating in the core.

Next, we discuss the possibility that systematic effects make 1H 1905+000 appear faint in quiescence whereas the true luminosity in quiescence is significantly higher. We shall show, however, that this is unlikely. If the distance is systematically underestimated the source luminosity may be higher. However, the distance for 1H 1905+000 is derived from the observed radius expansion burst peak flux. Kuulkers et al. (2003) have calibrated this distance estimation method comparing the distances derived from the burst peak fluxes of sources in globular clusters to the accurately known distances of those globular clusters. From their work it can be seen that if the composition of the burning material is known (hydrogen or helium rich burning material) the peak burst flux gives a reliable estimate of the distance (to within approximately 15 per cent). In ultra-compact systems hydrogen is likely depleted (Nelson et al. 1986; see Podsiadlowski et al. 2002 for a possible binary evolutionary

<sup>3</sup> 1H 1905+000 is only the third transient known to date that returned to quiescence after a long-duration outburst.

scenario leading to ultra-compact systems with some hydrogen still present). Therefore, it is save to assume that the radius expansion burst peak flux corresponds to the helium Eddington limit luminosity. In case of 1H 1905+000 this helium radius expansion burst limit on the distance is 10 kpc (see Jonker & Nelemans 2004). If however, hydrogen was present in the burning material the distance becomes smaller, making the upper limit on the quiescent luminosity more stringent still. The interstellar extinction,  $N_H$ , towards 1H 1905+000 is low compared to that found for most other low-mass X-ray binaries. From Einstein observations obtained when the source was in outburst Christian & Swank (1997) determined that the  $N_H$  to 1H 1905+000 is  $(1.9 \pm 0.2) \times 10^{21} \text{ cm}^{-2}$ . Typically, for many SXTs it is found that the interstellar extinction probed by  $N_H$  is somewhat higher in outburst than in quiescence (Jonker & Nelemans 2004). For that reason it is unlikely that the neutron star quiescent luminosity is much higher but that the source is hidden from our view due to an interstellar extinction that is much larger than measured in outburst.

Previous observations of several accretion-powered millisecond X-ray pulsars in quiescence have also shown that many of those sources have a low quiescent luminosity (e.g. SAX J1808.4–3658, Campana et al. 2002, XTE J0929–314 and XTE J1751–305, Wijnands et al. 2005, XTE J1807–294, Campana et al. 2005). However, except for SAX J1808.4–3658, the distance estimates for these systems are uncertain which makes the quiescent luminosity uncertain as well. Although, in order for these systems to have a luminosity  $\sim 10^{33} \text{ ergs}^{-1}$ , i.e. similar to that observed for Aql X-1 and XTE J1709–267 (Rutledge et al. 2002a, Jonker et al. 2003), the distance has to be unrealistically large, e.g.  $\sim 40$  kpc for XTE J0929–314. The planned deep (300 ksec) *Chandra* X-ray observation of 1H 1905+000 will provide new constraints on or a measurement of the quiescent neutron star luminosity in this system.

## ACKNOWLEDGMENTS

Support for this work was provided by NASA through Chandra Postdoctoral Fellowship grant number PF3–40027 awarded by the Chandra X-ray Center, which is operated by the Smithsonian Astrophysical Observatory for NASA under contract NAS8–39073. PGJ further acknowledges support from NASA grant GO4–5033X fund number 16617404. PGJ, CGB and GN acknowledge support from the Netherlands Organisation for Scientific Research. This research was (partially) based on data from the ING Archive. We further acknowledge Tom Marsh for use of his software package MOLLY, Sergio Ilovaisky for providing the original pdf-image of the V–band finder chart of 1H 1905+000 published in Chevalier, Ilovaisky & Charles (1985), and Frank Verbunt for comments on a earlier version of the manuscript. The authors would like to thank the referee for his/her comments which improved the manuscript.

## REFERENCES

- Abramowicz, M. A., Kluźniak, W., Lasota, J.-P., 2002, A&A, 396, L31
- Baiko, D. A., Yakovlev, D. G., 1995, Astronomy Letters, 21, 702
- Bildsten, L., Chakrabarty, D., 2001, ApJ, 557, 292
- Brown, E. F., Bildsten, L., Rutledge, R. E., 1998, ApJ, 504, L95
- Brown, E. F., Bildsten, L., Chang, P., 2002, ApJ, 574, 920
- Campana, S., Stella, L., 2000, ApJ, 541, 849
- Campana, S., Israel, G. L., Stella, L., Gastaldello, F., Mereghetti, S., 2004, ApJ, 601, 474
- Campana, S., Ferrari, N., Stella, L., Israel, G. L., 2005, A&A, 434, L9
- Campana, S., et al., 2002, ApJ, 575, L15
- Chen, W., Shrader, C. R., Livio, M., 1997, ApJ, 491, 312
- Chevalier, C., Ilovaisky, S. A., 1990, A&A, 228, 115
- Chevalier, C., Ilovaisky, S. A., Charles, P. A., 1985, A&A, 147, L3
- Christian, D. J., Swank, J. H., 1997, ApJS, 109, 177
- Colpi, M., Geppert, U., Page, D., Possenti, A., 2001, ApJ, 548, L175
- Cox, A. N., 2000, Allen's astrophysical quantities, Allen's astrophysical quantities, 4th ed. Publisher: New York: AIP Press; Springer, 2000. Edited by Arthur N. Cox. ISBN: 0387987460
- Deloye, C. J., Bildsten, L., 2003, ApJ, 598, 1217
- Fender, R. P., Gallo, E., Jonker, P. G., 2003, MNRAS, 343, L99
- Gänsicke, B. T., Braje, T. M., Romani, R. W., 2002, A&A, 386, 1001
- Garcia, M. R., McClintock, J. E., Narayan, R., Callanan, P., Barret, D., Murray, S. S., 2001, ApJ, 553, L47
- Gehrels, N., 1986, ApJ, 303, 336
- Haensel, P., Zdunik, J. L., 1990, A&A, 227, 431
- Hameury, J.-M., Barret, D., Lasota, J.-P., McClintock, J. E., Menou, K., Motch, C., Olive, J.-F., Webb, N., 2003, A&A, 399, 631
- Heinke, C. O., Grindlay, J. E., Lugger, P. M., Cohn, H. N., Edmonds, P. D., Lloyd, D. A., Cool, A. M., 2003, ApJ, 598, 501
- in't Zand, J. J. M., et al., 2001, A&A, 372, 916
- Jonker, P. G., Nelemans, G., 2004, MNRAS, 354, 355
- Jonker, P. G., Méndez, M., Nelemans, G., Wijnands, R., van der Klis, M., 2003, MNRAS, 341, 823
- Jonker, P. G., Galloway, D. K., McClintock, J. E., Buxton, M., Garcia, M., Murray, S., 2004, MNRAS, 354, 666
- Jonker, P. G., Campana, S., Steeghs, D., Torres, M., Galloway, D. K., Markwardt, C. B., Chakrabarty, D., Swank, J., 2005, MNRAS, 3
- Juett, A. M., Chakrabarty, D., 2005, ApJ, 627, 926
- King, A. R., Wijnands, R., 2006, MNRAS, 366, L31
- Kitamura, H., 2000, ApJ, 539, 888
- Kong, A. K. H., McClintock, J. E., Garcia, M. R., Murray, S. S., Barret, D., 2002, ApJ, 570, 277
- Kraft, R. P., Mathews, J., Greenstein, J. L., 1962, ApJ, 136, 312
- Kuulkers, E., den Hartog, P. R., in't Zand, J. J. M., Verbunt, F. W. M., Harris, W. E., Cocchi, M., 2003, A&A, 399, 663
- Lewin, W. H. G., Li, F. K., Hoffman, J. A., Doty, J., Buff, J., Clark, G. W., Rappaport, S., 1976, MNRAS, 177, 93P
- McClintock, J. E., Horne, K., Remillard, R. A., 1995, ApJ, 442, 358

- Menou, K., Esin, A. A., Narayan, R., Garcia, M. R., Lasota, J., McClintock, J. E., 1999, *ApJ*, 520, 276
- Narayan, R., Yi, I., 1994, *ApJ*, 428, L13
- Narayan, R., Garcia, M. R., McClintock, J. E., 1997, *ApJ*, 478, L79+
- Nelson, L. A., Rappaport, S. A., Joss, P. C., 1986, *ApJ*, 304, 231
- Podsiadlowski, P., Rappaport, S., Pfahl, E. D., 2002, *ApJ*, 565, 1107
- Reid, C. A., Johnston, M. D., Bradt, H. V., Doxsey, R. E., Griffiths, R. E., Schwartz, D. A., 1980, *AJ*, 85, 1062
- Rieke, G. H., Lebofsky, M. J., 1985, *ApJ*, 288, 618
- Rutledge, R. E., Bildsten, L., Brown, E. F., Pavlov, G. G., Zavlin, V. E., 2002a, *ApJ*, 577, 346
- Rutledge, R. E., Bildsten, L., Brown, E. F., Pavlov, G. G., Zavlin, V. E., Ushomirsky, G., 2002b, *ApJ*, 580, 413
- Salpeter, E. E., van Horn, H. M., 1969, *ApJ*, 155, 183
- Schlegel, D. J., Finkbeiner, D. P., Davis, M., 1998, *ApJ*, 500, 525
- Seward, F. D., Page, C. G., Turner, M. J. L., Pounds, K. A., 1976, *MNRAS*, 175, 39P
- Strohmayer, T. E., Markwardt, C. B., Swank, J. H., in't Zand, J., 2003, *ApJ*, 596, L67
- Tomsick, J. A., Gelino, D. M., Kaaret, P., 2005, *ApJ*, 635, 1233
- Ushomirsky, G., Rutledge, R. E., 2001, *MNRAS*, 325, 1157
- van Paradijs, J., McClintock, J. E., 1994, *A&A*, 290, 133
- van Paradijs, J., McClintock, J. E., 1995, p. 58 in X-ray Binaries, eds. W.H.G. Lewin, J. van Paradijs, and E.P.J. van den Heuvel, Cambridge: Cambridge Univ. Press
- van Paradijs, J., Verbunt, F., Shafer, R. A., Arnaud, K. A., 1987, *A&A*, 182, 47
- Verbunt, F., van den Heuvel, E., 1995, Formation and evolution of neutron stars and black holes in binaries, eds Lewin, van Paradijs, van den Heuvel, ISBN 052141684, Cambridge University Press, 1995.
- Wagner, R. M., Starrfield, S. G., Hjellming, R. M., Howell, S. B., Kreidl, T. J., 1994, *ApJ*, 429, L25
- Wijnands, R., Miller, J. M., Markwardt, C., Lewin, W. H. G., van der Klis, M., 2001, *ApJ*, 560, L159
- Wijnands, R., Guainazzi, M., van der Klis, M., Méndez, M., 2002, *ApJ*, 573, L45
- Wijnands, R., Homan, J., Miller, J. M., Lewin, W. H. G., 2004, *ApJ*, 606, L61
- Wijnands, R., Homan, J., Heinke, C. O., Miller, J. M., Lewin, W. H. G., 2005, *ApJ*, 619, 492
- Yakovlev, D. G., Pethick, C. J., 2004, *ARA&A*, 42, 169
- Yakovlev, D. G., Urpin, V. A., 1980, *Soviet Astronomy*, 24, 303
- Yakovlev, D. G., Kaminker, A. D., Levenfish, K. P., 1999, *A&A*, 343, 650
- Yakovlev, D. G., Levenfish, K. P., Haensel, P., 2003, *A&A*, 407, 265
- Yakovlev, D. G., Levenfish, K. P., Gnedin, O., 2005
- Zacharias, N., Urban, S. E., Zacharias, M. I., Wycoff, G. L., Hall, D. M., Monet, D. G., Rafferty, T. J., 2004, *AJ*, 127, 3043
- Zavlin, V. E., Pavlov, G. G., Shibanov, Y. A., 1996, *A&A*, 315, 141